
Cosmic Ray Propagation and Acceleration

Igor V. Moskalenko

NASA/Goddard Space Flight Center, Code 661, Greenbelt, MD 20771, USA

JCA/University of Maryland, Baltimore County, Baltimore, MD 21250, USA

Abstract

Theoretical views on particle acceleration in astrophysical sources and propagation of cosmic rays (CR) depend very much on the quality of the data, which become increasingly accurate each year and therefore more constraining. On the other hand, direct measurements of CR are possible in only one location on the outskirts of the Milky Way and present only a snapshot of very dynamic processes. The theoretical papers presented during the conference offer exciting insights into the physics of cosmic accelerators and processes which underlie the measured abundances and spectra of CR species.

This paper is based on a rapporteur talk given at the 28th International Cosmic Ray Conference held on July 31–August 7, 2003 at Tsukuba. It covers the sessions OG 1.3 Cosmic ray propagation, OG 1.4 Acceleration of cosmic rays, and a part of HE 1.2 Theory and simulations (including origins of the knee).

1. Introduction

The reviewed material can be organized as follows. OG 1.3 session (22 papers) covers production and propagation of light secondary isotopes, antiprotons and antinuclei, TeV electrons in CR and their sources, new effects in CR propagation, and new propagation models and codes. OG 1.4 session (15 papers) is mainly devoted to particle acceleration in non-relativistic shocks in supernova remnants (SNRs), Galactic winds, and galaxy clusters, and particle acceleration in relativistic shocks, jets, and pair plasmas. The reviewed part of HE 1.2 session (8 papers) discusses the origin of the “knee” as the result of diffusion or acceleration by *Galactic* sources, while the rest of the session is covered in the rapporteur talk by Takita [23]. Although the number of papers to review is relatively large, the subject, which can be broadly described as “theoretical astrophysics”, dictates an individual (not statistical) approach since every contribution is different. A complete and comprehensive discussion of all the results presented during the conference, however, is not attempted here due to space limitations. I thus offer my apologies to the authors who feel their work is not given sufficient coverage. The preference will be given to new ideas and results interesting to the CR com-

munity, while the choice necessarily reflects the Rapporteur’s personal view of the subject. This delicate matter is complicated by my own authorship of five contributed papers in session OG 1.3; those papers I attempt to appraise without a personal bias. The citation scheme adopted here identifies contribution papers by the first author name, session, and the page number.

2. Propagation of Low-Energy Cosmic Ray Nuclei

Acceleration of particles in the sources and their propagation in the interstellar medium are traditionally separated subjects, although there is no clear division between the “sources” and the “interstellar medium”. Under sources people usually intend SNRs, whose energetics can sustain the observed CR density, but the wider context includes also pulsars, stellar winds, and ensembles of shocks in superbubbles. Particles escaping the acceleration sites continuously (pulsars, winds, superbubbles) or on a short time scale (SNRs) are injected into the interstellar medium (ISM) and become what we call CR. Because of the huge Galactic volume, the CR particles remain contained in the ISM for some 10 Myr before escaping into intergalactic space. Energy losses and stochastic re-acceleration by magnetic turbulence (2nd order Fermi acceleration) during the propagation as well as escape from the Galaxy change the initial spectrum of particles. The destruction of primary nuclei via spallation gives rise to secondary nuclei and isotopes which are rare in nature, antiprotons, and pions which decay producing γ -rays and secondary positrons and electrons.

The wealth of information contained in the CR isotopic abundances makes it possible to study various aspects of their acceleration and propagation in the interstellar medium as well as the source composition. Stable secondary nuclei tell us about the diffusion coefficient and Galactic winds (convection) and/or re-acceleration in the interstellar medium. Long-lived radioactive secondaries provide constraints on global Galactic properties such as, e.g., the Galactic halo size. Abundances of K-capture isotopes, which decay via electron K-capture after attaching an electron from the ISM, can be used to probe the gas density and acceleration time scale. Details of the Galactic structure, such as the non-uniform gas distribution (spiral arms, the Local Bubble), radiation field and magnetic field (regular and random) distributions, and close SNRs may also affect the local fluxes of CR particles. Heliospheric influence (modulation) changes the spectra of CR particles below $\sim 10 - 20$ GeV/nucleon as they propagate from the boundaries of the solar system toward the orbits of the inner planets; these distorted spectra are finally measured by balloon-borne and satellite instruments. Current heliospheric modulation models are based on the solution of Parker’s transport equation [18] and include four major processes: convection, diffusion, drifts, and adiabatic energy losses. Individually, these processes are well studied, however, their combined effect, which produces the modulation, is still not fully understood.

The most frequently used “force-field” approximation [7] with one parameter, the modulation potential, accounts only for the effect of adiabatic losses. It has been recently realized that direct information about the fluxes and spectra of CR in distant locations is provided by the Galactic diffuse γ -rays, therefore, complementing the local CR studies, but this connection requires extensive modeling and is yet to be explored in detail.

Most efforts in OG 1.3 session are traditionally devoted to interpretation of the data in the few hundred MeV to GeV energy range, such as abundances of radioactive isotopes, light elements, spectrum of antiprotons, and predictions of antinuclei and exotic particles in CR.

2.1. Radioactive Secondaries

A conventional way to derive the propagation parameters is to fit the secondary/primary ratio, e.g., B/C. While taken alone the stable secondary/primary ratio does not allow one to derive a unique set of propagation parameters; the radioactive isotope abundances, e.g., $^{10}\text{Be}/^9\text{Be}$ ratio, are used to break the degeneracy. The propagation parameters can be derived in a semi-phenomenological approach, similar to what was used for decades in the Leaky-Box model, by adjusting the energy dependence of the diffusion coefficient *ad hoc* to fit the B/C ratio, or by using a proper diffusion model (including, e.g., diffusive reacceleration, convection) with corresponding fitting of free parameters to match the B/C ratio. While the formal procedure is quite clear, the nuclear production cross section errors introduce considerable uncertainty into the propagation parameters. Hundreds of isotopes are involved in the calculation of nuclear fragmentation and transformation of energetic nuclei in the course of their interaction with interstellar gas, however, the widely used semi-phenomenological systematics have typical uncertainties of the order of 20%, and can sometimes be wrong by a significant factor.

A steady state propagation model with cylindrical symmetry was used by Molnar & Simon (OG 1.3, p.1937) to study the abundance of ^{10}Be in CR, where the rigidity dependence of $D(R)/H$ (the ratio of the diffusion coefficient to the halo size, R being the rigidity) is derived *ad hoc* from the fitting to the B/C data. The low-energy data < 150 MeV/nucleon from Voyager, Ulysses, and ACE (to name only recent experiments) on $^{10}\text{Be}/^9\text{Be}$ ratio are all consistent and require the halo size $H \sim 4$ kpc, while the ISOMAX-98 data at energies around 1 GeV/nucleon lie higher than predicted by models. The authors offer two explanations to solve the discrepancy: cross section errors and the energy dependence of the halo size. The reaction $^{11}\text{B} + \text{p} \rightarrow ^{10}\text{Be}$ is one of the most important channels of ^{10}Be production, but four available data points hardly allow for any meaningful conclusion on the cross section; a change in the cross section from 5 to 25 mb above 1 GeV/nucleon consistent with the cross section error bars improves

the agreement with the ISOMAX data. The halo size also affects the $^{10}\text{Be}/^9\text{Be}$ ratio. In particular, the calculated ratio increases as the halo size decreases, an effect connected with the decrease of the effective collecting volume of CR (so that the produced radioactive species have less time to decay). The halo size, which decreases with energy, can thus improve the model. The interpretation of the latter effect is not, however, straightforward. On one hand, as the energy of the particles increase, they are less scattered by the magnetic turbulence in the halo and should escape faster to intergalactic space. On the other hand, in a model with a Galactic wind, the halo size should increase with energy (Völk, in the discussion) as low-energy particles are convected easier and thus never return, while high energy particles may still return. More accurate data from PAMELA and AMS will provide a conclusive test.

Papers by Donato et al. (OG 1.3, p.1953) and Farahat et al. (OG 1.3, p.1957) discuss the effect of the Local Bubble (LB) on the propagation of radioactive isotopes. The LB is a low density region around the sun, filled with hot HI gas (e.g., [21]). The size of the region is about 200 pc, and it is likely that it was produced in a series of supernova (SN) explosions. While this relatively small structure may produce only minor effects on stable nuclei, the radioactive isotopes may be underproduced in this region. Four radioactive isotopes, ^{10}Be , ^{26}Al , ^{36}Cl , and ^{54}Mn , are commonly used to probe the effective Galactic volume filled with CR and derive the confinement time of CR in the Galaxy. Their half-lives range from 3.07×10^5 yr (^{36}Cl) to 1.60×10^6 yr (^{10}Be) with the shortest half-life being most sensitive to the local structure. The half-life of $^{54}\text{Mn}(\beta^-)$ is the only one of the four which is not measured directly and remains the most uncertain. Assuming that the diffusion coefficient in the LB is equal to the Galactic average, the effect is easy to estimate: the calculated propagation lengths of these radioactive species appear to be comparable to the LB size. Inclusion of the LB into a model thus should lower the halo size compared to calculation without the LB. This simple picture is undermined by the fact that the propagation parameters (and the diffusion coefficient) in the LB are unknown while those derived from the B/C ratio give an *average* diffusion coefficient, which samples a large Galactic volume. A semi-analytical propagation model (with reacceleration *and* convection) and a formal χ^2 fit to the B/C, $^{10}\text{Be}/^9\text{Be}$, and $^{36}\text{Cl}/\text{Cl}$ ratios were used by Donato et al., who found that taken together the ratios are compatible with ACE data if the LB hole radius is $r_{\text{hole}} \sim 60 - 100$ pc, while $r_{\text{hole}} = 0$ is disfavored. The diffusion coefficient index treated as a free parameter was found to be $\delta = 0.5 - 0.8$. The latter is apparently larger than in conventional models with reacceleration, and besides, explaining the CR anisotropy measurements at high energies (see Fig. 1.) may be problematic. The $^{26}\text{Al}/^{27}\text{Al}$ ratio calculated in the same model was found to be inconsistent with the ACE data and marginally consistent with Ulysses data, which the authors conclude may indicate some errors in the data

(nuclear or astrophysical) used in the analysis. Indeed, the cross section errors are often the reason for inconsistency in propagation models. For Al isotopes the main progenitor is ^{28}Si , while the contribution of ^{27}Al to ^{26}Al is also important. For isotopes of Cl the main progenitor is ^{56}Fe , but the contribution of many lighter nuclei is equally important. Comparison with the data for those reaction channels shows that the semi-phenomenological approximations produce bad fits (e.g., [15,24]). A difference in the calculated $^{26}\text{Al}/^{27}\text{Al}$ and $^{36}\text{Cl}/^{35}\text{Cl}$ ratios at low energies in models with/without the LB has been also reported by Farahat et al., who used a Markov stochastic method to calculate the path-length probability distribution, followed by a weighted slab calculation.

2.2. *Light Stable Secondary Isotopes*

Isotopes of light elements in CR are almost all secondaries produced in spallations of heavier nuclei on interstellar gas Galaxy-wide, and their abundances reflect the propagation history of CR; an example is the best-measured B/C ratio, which is used to fix propagation parameters. On the other hand, weak local sources, e.g., old SNRs in the LB, may still accelerate particles out of the ISM by weak shocks [4] adding to the Galactic CR at low energy. This may change the local CR composition of progenitor nuclei adding a fresh local “unprocessed” component. Deviations of the calculated abundances of secondaries from measurements thus can tell us about our local environment. A study of the abundances of light elements, ^2H , ^3He , Li, Be, B, in reacceleration models with/without the LB has been reported by Moskalenko et al. (OG 1.3, p.1917), who use the GALPROP propagation code. Apparently both reacceleration models with/without the LB are consistent with the ACE data given the large error bars. $^3\text{He}/^4\text{He}$ ratio agree well with IMAX92 data indicating that ^3He in CR is mostly secondary. The He/Si ratio in the LB sources required to match the $^3\text{He}/^4\text{He}$ ratio is 2 times that of the Galactic CR sources indicating that the material was possibly diluted in the LB medium before the acceleration. Presented were also calculations of the $^2\text{H}/^4\text{He}$ ratio, which is a factor of 1.5 less than the IMAX92 value, but this may be connected with systematic errors in the data.

The deuteron flux as evaluated in simplified propagation models is presented by Sina et al. (OG 1.3, p.1973). The models (Leaky-Box, convection with a constant wind speed, and stochastic reacceleration) indicate somewhat different behavior of the flux below 1 GeV/nucleon. The calculations are consistent within a factor of 2 or less with the BESS data taken in a series of flights during different periods of solar activity. The reacceleration model generally agrees better with the data predicting the deuteron flux (modulation potential $\Phi = 500$ MV) just above the BESS-97 solar minimum data. Though, the modulation level can be deduced from the CR data and neutron monitors only approximately, the increased levels of modulation will result in a decrease of deuteron flux consistent with the

general trend, while other models would underestimate the deuteron flux.

Stable CR species probe a large region of the Galaxy. The size of this region depends essentially on the nuclear disintegration cross section and is smaller for heavier nuclei. A regular Galactic magnetic field may cause preferential propagation in azimuthal direction making some sources more important even if they are more distant. The global structure of Galactic magnetic field is currently derived from observations of rotation measures of more than 500 pulsars [8]. It is best described by two distinct components, a bi-symmetric spiral field in the disk with reversed direction from arm to arm, and an azimuthal field in the halo with reversed directions below and above the Galactic plane. Codino & Plouin (OG 1.3, p.1977) present their simulations of the propagation of CR particles from an acceleration site to the solar system. They show that the sources contributing to the local CR flux are predominantly located along the principal magnetic field line. Contrary to the Leaky-Box assumption, the mean trajectory length of CR particles reaching the solar system decreases with the increase of the atomic number and reaches a constant level of about 150 kpc for $A > 30$ at 10 GeV/nucleon.

Errors in the nuclear production cross sections are frequently quoted by many authors as one of the main reasons for uncertainty in propagation parameters, which are usually derived using B/C and $^{10}\text{Be}/^9\text{Be}$ ratios. This clearly becomes a factor hindering further progress since the accuracy of the cross sections used in astrophysics is far behind the accuracy of recent CR measurements. The scarce cross section data alone cannot be used to produce a reliable evaluation of the cross sections, while current nuclear codes and semi-empirical parameterizations also fall short of predicting cross section behavior for the whole range of target nuclei and incident energies. An auxiliary paper by Moskalenko & Mashnik (OG 1.3, p.1969) uses a collection of cross section data from LANL nuclear database to evaluate the most important channels of production of Li, Be, and B isotopes. The individual cross section evaluations are tested against isobaric and cumulative data where available. Such work should help to eventually reduce the discrepancy in the results of different groups.

2.3. *Secondary Antinuclei*

The baryonic asymmetry of the universe is one of the most intriguing puzzles. Antinuclei in CR may present an opportunity to test the baryonic asymmetry or uncover evidence for annihilation of the non-baryonic Dark Matter particles (weakly interacting massive particles – WIMPs) whose existence is predicted by supersymmetric models [12]. The absence of baryonic antimatter in the universe or its presence in equal amounts with matter in spatially separated domains, if found, would have a dramatic impact on theories of grand unification, Big Bang nucleosynthesis, and cosmology. The lower limit to the domain size perhaps corresponds to the scale of a galaxy cluster, of the order of 20 Mpc, because the

intercluster voids can prevent annihilation. Due to the very low probability of formation of *secondary* antinuclei in CR, the detection of an antinucleus with $Z < -1$ in CR would be a “smoking gun” of new physics. The production of secondary antinuclei \bar{d} , \bar{t} , ${}^3\bar{\text{He}}$, ${}^4\bar{\text{He}}$ in the atmosphere and in CR interactions with interstellar gas has been evaluated by Baret et al. (OG 1.3, p.1961), who used a coalescence model. The coalescence model is based on the hypothesis that nucleons produced in collisions of energetic particles fuse into light nuclei whenever the momentum of their relative motion is smaller than the coalescence radius in momentum space. Galactic propagation has been evaluated using the Leaky-Box and diffusion models. The atmospheric background of antinuclei is shown to be considerably less than the secondary antinuclei flux in CR thus does not contribute much to the experimental uncertainty in searches for antimatter nuclei in CR. In the search for primordial antimatter ${}^4\bar{\text{He}}$ is a good candidate because of the vanishing background of secondary particles.

The indirect searches for exotic sources such as WIMPs or primordial black holes also concentrate on signals in CR with low background. The most often discussed are searches for spectral signatures in antiprotons, positrons, and diffuse γ -rays. Secondary antiprotons and positrons (and diffuse γ -rays) are products of interactions of mostly CR protons and helium nuclei with interstellar gas. Due to the kinematics of pp -interactions, the spectrum of antiprotons peaks at about 2 GeV decreasing sharply toward lower energies, a unique shape distinguishing it from other CR species. If the CR propagation model and heliospheric modulation is correct, a model that describes any secondary to primary ratio should equally well describe all the others: B/C, sub-Fe/Fe, \bar{p}/p ratios, as well as spectra of nuclei, positrons, and diffuse Galactic continuum γ -rays. It appears that relatively simple propagation models can not account simultaneously for the nuclei component in CR and antiprotons. In particular, a “standard” reacceleration model pose a problem since it produces too few antiprotons* [14,16] though it works well for other CR species.

Moskalenko et al. (OG 1.3, p.1921) discuss the reasons for the deficit of antiprotons as calculated in the reacceleration model. The uncertainties are described and divided into four categories: propagation models and parameters, production cross sections of isotopes and antiprotons, heliospheric modulation, and systematic errors of measurements. In the first category, the most uncertain are the spectra of CR species in the distant regions of the Galaxy; a direct test is provided by diffuse γ -rays, but the message of the “GeV excess” [10] is not fully understood yet. Nuclear production cross section errors are one of the major concerns; while there are not enough measurements, semi-empirical systematics are often wrong by 20% and sometimes by a considerable factor (for more details see Sections 2.1. and 2.2.). The errors introduced by heliospheric modulation and

*For an alternative viewpoint see [5].

instrumental errors are difficult to account for, but their effect could be reduced by careful choice of data. If, however, interstellar propagation and heliospheric modulation are correct, the discrepancy may indicate new phenomena. The paper discusses new ideas such as the change in the character of the diffusion at low energies, the effect of the local environment (e.g., fresh low-energy CR nuclei from the Local Bubble), and a population of low-energy proton sources, etc. New accurate measurements of antiprotons and CR at both low and high energies can help to resolve the issue.

2.4. *New Approaches to CR propagation*

Galactic CR are an essential factor determining the dynamics and processes in the ISM. The energy density of relativistic particles is about 1 eV cm^{-3} and is comparable to the energy density of the interstellar radiation field, magnetic field, and turbulent motions of the interstellar gas. While propagation of CR is often considered as propagation of test particles in given magnetic fields, the stochastic acceleration of CR by MHD waves causes damping of waves on a small scale, which, in turn, affects the propagation of CR. This illustrates a need for a self-consistent approach employed by Ptuskin et al. (OG 1.3, p.1929) who develop a formalism for the dissipation of hydromagnetic waves on energetic particles for the cases of Kolmogorov $W(k) \propto k^{-5/3}$ and Iroshnikov-Kraichnan $W(k) \propto k^{-3/2}$ spectra of the turbulences. In this formalism the mean free path of CR particles depends not only on the spectrum of turbulences, but also on the CR (mostly protons) momentum distribution function itself. The Kolmogorov type cascade is not very much affected by the damping. The Iroshnikov-Kraichnan type cascade is significantly affected; this should lead to a modification of CR transport below $\sim 10 \text{ GeV/nucleon}$. In particular, the diffusion coefficient will increase toward low energies, an effect used *ad hoc* in the Leaky-Box model. This qualitative analysis is confirmed by numerical calculations by Moskalenko et al. (OG 1.3, p.1925), who employed the GALPROP propagation code and used an iterative numerical procedure starting from an undisturbed diffusion coefficient. It offers a new explanation of the peak in the secondary/primary ratio at a few GeV/nucleon: because of the damping, the amplitude of short waves is small and thus the low energy particles rapidly escape the Galaxy without producing secondaries. The preliminary analysis shows that inclusion of the damping allows one to reproduce the B/C ratio and obtain a good agreement with spectra of CR nucleons using a unique power-law injection spectrum. Another interpretation, that the peak is produced by CR reacceleration [20] on an undisturbed Kolmogorov-type spectrum, remains as a viable alternative.

2.5. Propagation Models and Codes

Though the main features of CR propagation in the Galaxy seem to be well established [3], some simplifications and inconsistencies remain. The usual approach is to impose Galactic boundaries beyond which particles escape freely. Hareyama et al. (OG 1.3, p.1941, p.1945) and Shibata et al. (OG 1.3, p.1949) develop an analytical model of a boundary-less Galaxy, where the boundaries are replaced with exponential forms of the diffusion coefficient, gas density, and sources, both in R and z . The particle energy change (energy losses, reacceleration, convection) is neglected. The spectra of primaries and B/C and (Sc+Ti+V)/Fe ratios are reproduced above 5 GeV/nucleon given a set of fitting parameters; $^{10}\text{Be}/^9\text{Be}$ ratio is also calculated.

While analytical methods explore new approaches, numerical methods offer realistic treatment of CR propagation and calculation of many CR species simultaneously in the same model. Such approach takes advantage of independent constraints from many different kinds of data. The choice and optimization of a numerical scheme is the first necessary step in the development of a new propagation code. Busching et al. (OG 1.3, p.1981, p.1985) test a modified leapfrog/DuFort-Frankel scheme. A simplified time-dependent transport equation (cylindrical symmetry) has been expanded using Bessel functions in r and trigonometrical functions in φ , where the particle momentum is treated as a parameter. This reduces it to a system of time dependent 1-D equations for the expansion coefficients, which is solved numerically. The authors present simulations of the intensity variation of CR density (at 10 GeV/nucleon) during a period of 10 Myr in a cell of $500 \text{ pc} \times 500 \text{ pc}$ containing a SNR.

GALPROP is a well-developed realistic numerical model of CR propagation, which is used in numerous applications. The source code (C++) is regularly updated and posted on the Web together with output FITS files (models). However, reading the FITS format requires some programming and may apparently be not convenient for everyone. Moskalenko et al. (OG 1.3, p.1925) are developing a Web-based interface for the GALPROP models that supports various formats. The interface will include a simple form in the Web browser while the output results will be provided as computer readable tables and graphics files. For every posted model a user may request any of the following: spectra of any combination of isotopes or elements $Z \leq 28$, arbitrary isotopic ratios vs. kinetic energy, isotopic distribution for a given Z , elemental and isotopic abundance at arbitrary energy, as well as antiprotons, electrons and positrons. First, it will be available for the solar vicinity and later for the whole Galaxy.

3. Local Sources and TeV Electrons

In studies of cosmic-ray propagation and diffuse continuum γ -ray emission from the Galaxy it has usually been assumed that the source function can be

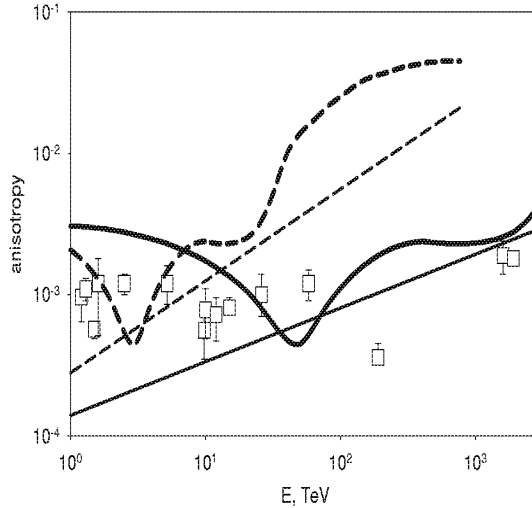


Fig. 1. The CR anisotropy produced by local supernovae (thick curves) and the expected fluctuation anisotropy (thin straight lines) in the reacceleration (solid curves) and the plain diffusion (dashed curves) models (Ptuskin et al., OG 1.3, p.1933).

taken as smooth and time-independent, an approximation justified by the long residence time ($> 10^7$ years) of cosmic rays in the Galaxy. However, the inhomogeneities have observable consequences, and their study is a step toward a “realistic” propagation model based on Galactic structure and plausible source properties. The random nature of CR sources leads to fluctuations of CR intensity in space and time. Ptuskin et al. (OG 1.3, p.1933) study the effect of nearby SNRs on the CR anisotropy at 1–1000 TeV where the energy losses of protons and heliospheric modulation are not important. In the case of distributed sources, the anisotropy calculated in the reacceleration model with the diffusion coefficient $D \propto E^{0.3}$ agrees better with the data above ~ 10 TeV than in the plain diffusion model ($D \propto E^{0.54}$), which is a standard result. Inclusion of nearby SNRs improves the agreement of the data with the reacceleration model, where the most important contributions come from Vela and S 147 (Fig. 1.). Inclusion of a very young and close SNR RX J0852.0–4622 (0.2 kpc, 700 yr) would dramatically change the predicted anisotropy; however it is probable that the source is still in a free expansion stage with accelerating particles confined inside the remnant.

For electrons at very high energies, where the energy losses due to inverse Compton and synchrotron emission are rapid, the effect of the stochastic nature of CR sources becomes even more apparent. Swordy (OG 1.3, p.1989) and Yoshida et al. (OG 1.3, p.1993) discuss fluctuations of TeV electrons due to nearby SNRs. For the typical energy density of Galactic radiation and magnetic fields of 1 eV cm^{-3} , the energy loss timescale is $\sim 3 \times 10^5 \text{ yr}$ at 1 TeV, and becomes as short as $\sim 3 \times 10^3 \text{ yr}$ at 100 TeV. A cutoff in the electron spectrum at very high energies is thus unavoidable because of both large energy losses and a discrete nature of

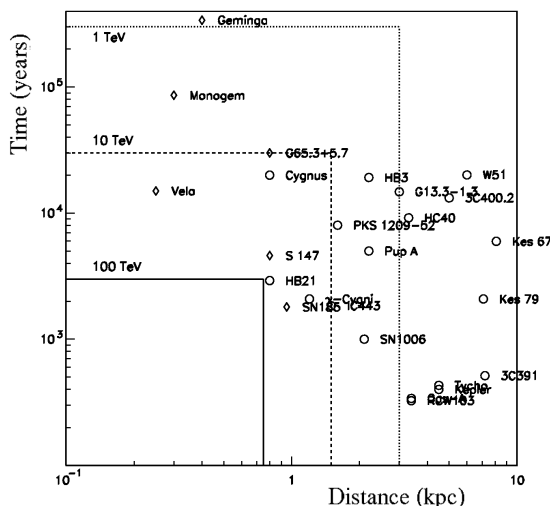


Fig. 2. Compilation of nearby shell-type and plerion SNR distances and ages. Line boxes represent limiting energies for electrons to reach Earth (Swordy, OG 1.3, p.1989).

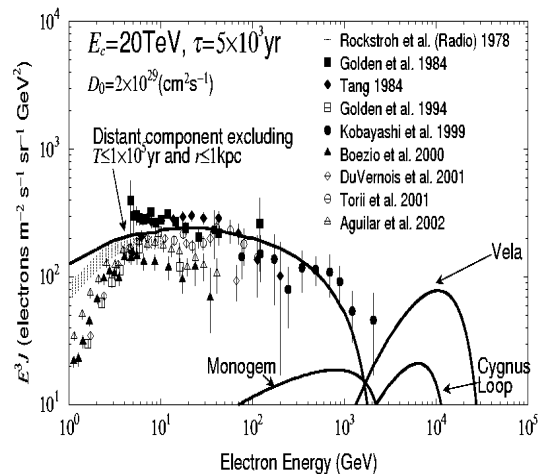


Fig. 3. The local electron spectrum with estimated contributions of nearby sources. The source spectrum has a cut-off at 20 TeV, $\tau = 5$ kyr (Yoshida et al., OG 1.3, p.1993).

the sources. This is similar to the GZK effect for ultra high energy CR, but it should be observable in the electron spectrum at much lower energies (though a smaller flux of secondary electrons should be present in CR at all energies). The analysis of nearby shell-type SNRs has shown that the electron spectrum should have a cut off between 30 TeV and 100 TeV as measured near the solar system (Fig. 2.). Yoshida et al. continue earlier studies of the propagation of very-high-energy electrons from local sources by Nishimura and collaborators. Their calculations predict that some nearby SNRs are possibly capable of producing unique identifiable features in the CR electron spectrum at 1–30 TeV (Fig. 3.), where the important parameters are the distance and the age of a SNR. The most promising candidate sources of TeV electrons are Vela, Cygnus Loop, and Monogem. Very-high-energy electron measurements give a direct test of SNR origin of CR, but also an important test of our local environment. The features in the electron spectrum and the cutoff energy would immediately signal which SNR(s) is/are affecting the local CR flux and to what degree with implications for Galactic CR propagation models.

A study of two types of formalism for second-order Fermi acceleration [9,20] in the interstellar medium is presented by Komori (OG 1.3, p.1997). It shows that the approaches are almost identical in the case of the same energy gain by a particle. The study concludes that the consistency with the *local* spectrum of CR electrons in reacceleration models requires a break at ~ 10 GeV in the electron source spectrum. Since the local spectrum is affected by the solar modulation, it is worth comparing with the spectral index of the *interstellar* electron spectrum.

The latter can be deduced from observations of synchrotron spectral index and intensity; the synchrotron emission in 10 MHz – 10 GHz band constrains the electron spectrum in the $\sim 1 - 10$ GeV range. Indeed, the low-frequency index $\beta \lesssim 2.5$ [19] indicates that the index of the injection spectrum must be below ~ 2.0 . Casadei & Bindi (OG 1.3, p.2001) discuss the local spectrum of electrons between 0.8 GeV and 2 TeV. They use a collection of electron CR measurements renormalized to the same value at 20 GeV. The fit shows that such spectrum can be represented by a power law in kinetic energy with index 3.4. A model with a single source also provides a good fit to the data above 10 GeV.

4. Particle Acceleration in Shocks

Shock acceleration is viewed as a “universal” acceleration mechanism working well on different scales and in different astrophysical environments [11]. The non-relativistic shocks are formed where the pressure of a supersonic stream of gas drops to the much lower value of the environment. Examples of non-relativistic shocks include the Earth’s bow shock, solar wind termination shock, shocks in expanding SN shells, and galactic wind termination shocks, to name only a few. The relativistic shocks give rise to nonthermal particles populations in astrophysical plasma known to exist in cores and jets of active galactic nuclei and quasars, and probably existing in blast waves of γ -ray bursts. The early results were obtained in the test-particle approximation, where the test particles do not modify the shock. If acceleration is efficient, a considerable amount of energy is transferred to the accelerated particles and they then act on the shock itself, dynamically modifying it. A significant flux of energetic particles against cold material will generate plasma turbulence. Escape of high-energy particles from the shock will allow the shock compression ratio to increase, which flattens the spectrum of accelerated particles. The non-linear effects are important in SNR because of the strong shocks and long expansion time. It is usually assumed that the Bohm diffusion coefficient is a good approximation for strong shocks. Important parameters are the angle α between the shock normal and the upstream magnetic field and $M_A = V/v_A$ Alfvén Mach number, where V is the shock speed, and v_A is the Alfvén speed. The characteristic feature of the shock acceleration is the formation of a power-law spectrum of accelerated particles in rigidity.

The papers in OG 1.4 section discuss particle acceleration in SNRs, reacceleration of high-energy particles by shocks in the Galactic wind, acceleration by shocks from mergers of galaxy clusters, shock waves due to the formation of the large scale structure of the universe, and relativistic shocks.

4.1. *Non-Relativistic Shocks*

The major sources of CR are believed to be SNe and SNRs with some fraction coming from pulsars, compact objects in close binary systems, and stellar winds. Observations of X-ray and γ -ray emission from SNRs reveal the presence of energetic electrons thus testifying to efficient acceleration processes near these objects, while evidence of accelerated hadrons is yet to be found. The radiation produced by an SNR depends on the electron spectrum *inside* the SNR. Lipari & Morlino (OG 1.4, p.2027) calculate the spectra of electrons and protons *inside* young SNRs. Their solution for protons gives a standard spectrum with power-law index 2. Inclusion of energy losses for electrons due to synchrotron emission and inverse Compton scattering on cosmic microwave background naturally produces a cut off in the electron spectrum. They argue that there are two different populations of electrons, those in the “accelerator” and those which are in the “storage” inside the remnant shell. The latter are particles trapped in turbulent magnetic fields left behind the expanding shell. The two emission mechanisms, synchrotron and inverse Compton scattering, produce two peaks in the photon spectrum. The relative intensity of the peaks depends on the magnetic field strength inside the remnant. The lower field results in a larger flux of TeV photons, but also facilitates particle escape, reducing the intensity of a synchrotron peak. Hoshino & Shimada (OG 1.4, p.2047) use particle-in-cell simulations to study electron acceleration by a series of large amplitude electrostatic soliton-like waves excited by the Buneman instability in SNR shocks.

While SNRs are “conventional” sources of CR up to the knee energies $\sim 3 \times 10^{15}$ eV, the origin of higher energy particles remains unclear. Acceleration to higher energies may require new classes of sources or multiple shocks (for more details see Section 5.). Völk & Zirakashvili (OG 1.4, p.2031) argue that the knee must be a feature of the source spectrum. They propose CR *reacceleration* in a supersonic Galactic wind at distances 50 to 100 kpc from the plane as a mechanism to accelerate high-energy CR particles beyond the knee energies, up to $Z \times 10^{17}$ eV. The spiral compression of the wind formed due to the differential Galactic rotation and the differences in the wind speed will form a sawtooth series of forward shocks, which will re-accelerate high-energy particles from the disk by ~ 2 orders of magnitude. Some fraction of these particles returns to the disk plane giving rise to the component above the knee. The process is reminiscent of the so-called Corrotating Interaction Regions in the solar wind. There is no way in this mechanism to produce CR above 10^{18} eV. The energy gain in this process is very slow so the process of reacceleration may take some Myr.

The nonthermal radiation observed from some galaxy clusters implies the presence of accelerated particles in the intracluster medium. The acceleration by shocks formed due to cluster mergers and its implication for γ -ray emission from clusters is discussed in two papers, Blasi & Gabichi (OG 1.4, p.2051) and

Takizawa et al. (OG 1.4, p.2059). Blasi & Gabichi analysed the compression factors of the shocks based on a model of mergers and formation of the hierarchical structure of the universe. Their simulations indicate that particle acceleration by shocks associated with mergers of clusters is inefficient. The large majority of merger shocks have the Mach number below 2 with correspondingly low acceleration capability; this corresponds to particle spectra much steeper than required to explain the observed nonthermal radio emission. In the case of shocks formed due to the accretion in the gravitational field of the forming cluster, Mach numbers can reach several hundred, which results in the formation of a flat particle spectrum $\propto E^{-2}$. The calculation of the γ -ray emission due to inverse Compton scattering off the cosmic microwave background photons shows that future orbital γ -ray experiments, such as AGILE and GLAST, will be able to detect a few to several dozens of clusters. The overall contribution of clusters to the diffuse extragalactic γ -ray emission (as derived from EGRET data [22]) is about 10%, which is significantly lower than some other estimates. The cluster merger shocks and random Alfvén waves in intracluster space are also discussed by Takizawa et al., who used N-body/hydrodynamic simulations to study the electron spectral evolution due to acceleration by the shocks. The simulations show that accelerated electrons are mostly confined to the shocks and exhibit their morphology structure in radio and X-ray emission, while random Alfvén waves may produce the radio halo. Comparison with radio emission from the Coma cluster indicates that the Alfvén wave power spectrum may be significantly modified due to particle-wave interactions.

Three papers are devoted to simulation of CR acceleration in shocks emerging in the large scale structure formation of the universe. N-body/hydrodynamic simulations of formation of large scale structure by Ryu et al. (OG 1.4, p.2055) support scenarios in which the intracluster medium contains significant populations of CR. Cosmological shocks may be induced due to the accretion of baryonic gas onto the nonlinear structures, such as sheets, filaments, knots, subclump mergers, and chaotic flow motions. The simulations show that while shocks with Mach numbers up to 100 are possible, the majority of CR is accelerated by shocks with Mach number of a few. The mean separation between shock surfaces is $\sim 4h^{-1}$ Mpc at present. Kang & Jones (OG 1.4, p.2039) study CR injection and acceleration efficiency in quasi-parallel cosmic shocks in 1-D geometry for a wide range of Mach numbers and preshock conditions. They find that a fraction of $10^{-4} - 10^{-3}$ of the particles which passed through the shock becomes CR. A new fast numerical scheme for the time-dependent CR diffusion convection equation to study the evolution of CR modified shocks is being developed by Jones & Kang (OG 1.4, p.2035).

4.2. *Relativistic Shocks*

Relativistic shocks are associated with the most energetic objects in the universe, such as active galactic nuclei, quasars, and γ -ray bursts. The particle velocity in such shocks is comparable to the bulk velocity leading to substantial anisotropy of the angular distribution of particles. In case it makes an angle to the shock normal, the upstream magnetic field is strongly modified by the Lorentz transformation to the downstream frame and further modified by the shock compression. The downstream magnetic field is increased and tilted toward the plane of the shock influencing both the shock jump conditions and particle acceleration. The magnetic field intensity increases across the shock reflecting particles and thus provides more effective energy gain.

Relativistic shock acceleration was the subject of four papers, by Niemec & Ostrowski (OG 1.4, p.2015, p.2019), by Virtanen & Vainio (OG 1.4, p.2023), and by Nishikawa et al. (OG 1.4, p.2063). The process of first-order Fermi acceleration in the parallel and oblique shocks in a pair plasma in the presence of finite-amplitude magnetic field perturbations is discussed by Niemec & Ostrowski. The perturbations are assumed to have either a flat, $F(k) \sim k^{-1}$, or a Kolmogorov spectrum, $\sim k^{-5/3}$. In the case of a parallel shock, the long-wave finite-amplitude perturbations produce locally oblique magnetic field configurations with the probability of particle reflection depending on the turbulence amplitude. This leads to shorter acceleration timescales. In the case of an oblique shock, the exact shape of the spectrum depends on the amplitude of the magnetic field perturbations and the wave power spectrum. Subluminal shocks produce a spectrum that hardens below the cut-off energy, while superluminal shocks lead to a spectrum steepening below the cut-off. Electron acceleration in parallel shocks with finite thickness is studied by Virtanen & Vainio using test-particle simulations, where the thickness of the shock is determined by the ion dynamics. Electrons were injected in the downstream region. The finite thickness of the shock reduces its efficiency, leading to a modest acceleration resembling adiabatic compression. An energy-independent mean free path leads to a spectral index 3.2. The canonical value 2.2 is obtained in the case of a thin shock as a high energy limit for a mean free path increasing with energy. Nishikawa et al. present a simulation of particle acceleration and generation of the magnetic field in relativistic jets using 3-D relativistic particle-in-cell (REMP) simulations with and without initial ambient magnetic fields. They show that the Weibel instability is responsible for generating and amplifying highly nonuniform, small-scale magnetic fields, which contribute to the electron's transverse deflection behind the jet head, while accelerating particles parallel and perpendicular to the jet propagation vector. The deflected electrons emit “jitter” radiation which may help to understand the complex time evolution and/or spectral structure of γ -ray emission from astrophysical objects.

5. Origins of the Knee

The small change in the slope at $\sim 3 \times 10^{15}$ eV of otherwise almost featureless CR spectrum is known as the “knee.” Besides numerous speculations, the origin of this feature discovered more than 40 years ago by a group of scientists at Moscow State University still remains unexplained. Because of the low flux of CR particles at the knee energy, direct measurements from balloons and spacecraft are apparently inefficient; indirect measurements using the extensive air showers technique (Cherenkov light and detector arrays) is presently the only way to study CR with high statistics at energies near or above the knee. One of the main difficulties of the indirect techniques is that the event reconstruction depends on hadronic interactions at energies beyond those currently available in accelerator experiments. This leads to one possible explanation that the knee is the result of our incomplete understanding of the properties of high energy particle interactions. On the other hand, the knee position is remarkably close to the highest possible energy expected from the shock acceleration in SNRs. Acceleration of particles to energies beyond the knee still requires a satisfactory explanation. The ideas discussed consider new classes of Galactic or extragalactic sources, a local source, or acceleration by multiple shocks. Additionally, a drift of CR particles in the large scale regular Galactic magnetic field, Hall diffusion, may dominate the regular diffusion at very high energies thus making it possible to explain the knee by the increased leakage of CR from the Galaxy. Changes in the amplitude and phase of the anisotropy and/or a composition of CR at the knee region can perhaps provide necessary clues to its origin, although the current uncertainties in the composition are still large given the uncertainties in the underlying hadronic interaction models.

The HE 1.2 papers are devoted to the origins of the knee in CR spectrum and CR above the knee.

5.1. *Diffusion Mechanism*

The “poly-gonato” empirical model is proposed by Horandel et al. (HE 1.2, p.243), where the knee structure appears as the result of many knees in the individual CR components with cutoff energies proportional to the nuclear charge. Because the model fits the CR composition below and above the knee reasonably well, the authors speculate on the physical grounds of the model. While cutoffs of the individual components appear naturally as the result of shock acceleration in SNRs, Hall diffusion may dominate at high energies facilitating particle escape from the Galaxy due to drift effects and could provide more steepening above the knee. The structure of the regular magnetic field was chosen in the form proposed by Rand-Kulkarni in the disk and incorporates a large halo with symmetric or antisymmetric field configuration. Though the model reproduces the knee spectrum

of CR, it suffers from certain simplifications. Nuclear disintegration is neglected. The transport equation includes only diffusion and source terms with all sources located in a ring at 4 kpc from the Galactic center. With a wider distribution of the sources it may be difficult to explain the sharp knee structure.

Ogio & Kakimoto (HE 1.2, p.315) suggest that the knee structure can be explained by particle diffusion perpendicular to the Galactic plane due to the open magnetic field lines of loops and filaments. However, the advection velocity derived by the authors is apparently too large $\sim 500 \text{ km s}^{-1}$ and may conflict with that derived from low-energy CR.

The residence time of Galactic CR in the disk has been computed by Codino and Plouin (HE 1.2, p.319), who simulated some 10^8 particle trajectories originating in the disk. In their simulations, the probabilities of nuclear interactions and escape depend on the gas column density. The magnetic field structure adopted includes a regular spiral field in the disk and a random component, where the latter is responsible for chaotization of particle trajectories and escape. The obtained residence time depends on the nucleus charge and has a plateau (~ 2.2 Myr for carbon) between 10^{10} and 10^{14} eV decreasing toward higher energies. A second plateau appears above 10^{16} eV with the residence time comparable to a simple crossing time of the Galaxy.

5.2. Galactic Sources

Young SNRs are traditionally considered as the sites of CR acceleration by diffusive shocks. The conventional estimates put the maximum reachable particle energy at or just below the knee energy. Bell & Lucek [2] suggested that acceleration of CR particles in the shock is accompanied by simultaneous amplification of the magnetic field around the shock allowing for acceleration of particles to much higher energies. Given a possibility to increase the Alfvén Mach number in the shock to 10^3 the maximum possible particle rigidity can reach 10^{17} V. This mechanism is investigated by Drury et al. (HE 1.2, p.299) in a simplified “box model.” Assuming Bohm diffusion and a Sedov-Taylor expansion law, the characteristic curve in the momentum vs. time plane relates the final energies to the starting times. The authors indicate that under plausible conditions this mechanism produces a high-energy tail with a slope $4.25 + \delta$ which is slightly steeper than canonical value of 4 with a transition to the usual spectrum in the knee region.

A growing number of observations have yielded large statistics of SNe which come in various flavors: thermonuclear SNe Ia, core collapse SNe Ib,c, II (with subclasses), and exhibit a wide range of luminosities, expansion velocities, and chemical abundances. A new class of core collapse SNe Id seems to be found that is also called Ic “hypernovae” to underline their peculiar high expansion velocities and explosion energies. The observed differences in SN shell velocities and

energetics are translated into different efficiencies of particle acceleration and the corresponding distribution of maximum reachable energies of accelerated particles. This diversity of characteristics of SNe and their different frequencies are exploited by Sveshnikova (HE 1.2, p.307) to explain the knee structure as a superposition of SNRs of different types. Although the explosion energy distribution of SNe is not established, it can approximately be deduced from the absolute magnitude distribution. In this model, the knee structure is mainly composed of two types of SNe with type Ib,c contributing mostly below the knee and type II_n dominating above the knee. The fraction of events responsible for the formation of the knee is estimated at $\sim 2 \times 10^{-4} \text{ yr}^{-1}$ with a total energy of $\sim 30 \times 10^{51} \text{ erg}$ that might be identified with hypernovae. The predicted composition shows irregular behavior above the knee with a trend toward dominance of heavier nuclei. This obviously interesting hypothesis should be tested further. Given the enormous power of hypernova events and their low frequency, only a few of them would determine the spectrum of CR at the knee region. The consequences are a large anisotropy and large historical variations of CR intensity. An indication of four large increases of CR intensity during the last 150 kyr is indeed found, e.g., in studies of abundance of cosmogenic ^{10}Be in Antarctic ice [13], but their interpretation and identification with astrophysical objects are yet to be done.

The sharpness of the knee and the change in the anisotropy amplitude may be an argument toward a recent local SNR source, which adds a small component, the knee, on the top of a smooth Galactic CR spectrum. The explanation was originally proposed in a series of papers by Erlykin & Wolfendale (e.g., see [6]). Bhadra (HE 1.2, p.303) explores the possibility of a pulsar origin of the knee in a similar model. The author argues that the source of energetic particles nearby, if it exists, should be visible in γ -rays. A pulsar, such as Geminga or Vela, may thus be responsible for the fine knee structure, while the absence of the γ -rays from a SNR nearby can be explained by the low density environment of the source.

6. Miscellaneous

The miscellaneous section collects several papers, which are somewhat outside the traditional topics of CR acceleration and propagation. Kuwabara et al. (OG 1.3, p.1965) use 2-dimensional MHD simulations to study the effect of the Parker instability in the presence of CR. A Lagrangian formalism for the Fokker-Planck transport equation is proposed by Burgoa (OG 1.4, p.2011). Zenitani & Hoshino (OG 1.4, p.2043) discuss a magnetic reconnection and drift kink instability in electron/positron plasma as a source of nonthermal particles. Saito et al. (HE 1.2, p.311) investigate particle acceleration due to electrostatic shock wave driven by counterstreaming pair plasma with background magnetic field.

7. Wider Perspective

In the summary, it is appropriate to identify several topics expect to become the subject of intensive studies in coming years. At low energies, ACE, Ulysses, and Voyager continue to deliver excellent quality spectral and isotopic data, while there is no matching experiment at GeV energies. The most accurate data in the GeV range so far were obtained more than 20 years ago by the HEAO-3 instrument. Two generations of theorists have speculated on the origin of the sharp peak in the B/C ratio, one of the HEAO-3 results, eagerly awaiting new data. New accurate positron and especially antiproton measurements are desirable. Antiprotons with their unique spectral shape are seen as a key to many problems, such as Galactic CR propagation, possible imprints of our local environment, heliospheric modulation, dark matter etc. Happily, several high resolution space and balloon experiments are to be launched in the near future. PAMELA (launch in 2004) is designed to measure antiprotons, positrons, electrons, and isotopes H through C over the energy range of 0.1 to 300 GeV. Future Antarctic flights of a new BESS-Polar instrument will considerably increase the accuracy of data on antiprotons and light elements. AMS will measure CR particles and nuclei $Z \lesssim 26$ from GeV to TeV energies. This is complemented by measurements of heavier nuclei $Z > 29$ by TIGER. Several missions are planned to target specifically the high energy electron spectrum, which could provide unique information about our local environment and sources of CR nearby. They will also give necessary clues to the interpretation of the spectrum of diffuse γ -ray emission from the future GLAST mission capable of measuring γ -rays in the range 20 MeV – 300 GeV. In its turn, modeling the spectrum and distribution of the Galactic diffuse γ -ray emission gathered by GLAST will provide insights into the CR spectra in remote locations. Besides, GLAST with its high sensitivity and resolution should deliver a final proof of proton acceleration in SNRs – long awaited by the CR community. In the knee region and beyond, several satellite and ground-based instruments are planned to dramatically increase statistics and energy coverage (see rapporteur talks [1,17]). A breakthrough on supersymmetry and high-energy particle interactions should come with operation of the new CERN large hadronic collider, LHC.

In the past and at present, new studies and discoveries in CR physics provide a fertile ground for research in many areas of Astrophysics, Particle Physics, and Cosmology, such as the search for dark matter signatures, new particles and exotic physics, the origin of elements, the origins of Galactic and extragalactic γ -ray diffuse emission, heliospheric modulation etc. I am glad that this conference has been successful enough to gather new ideas and approaches and to show further horizons to the CR community.

8. Acknowledgments

I am grateful to the Organizing Committee for the invitation to be a rapporteur and for providing the financial support as well as for their thorough preparation of the conference. I would like to thank all the contributing authors for their patient answers to my numerous questions. I am also indebted to Vladimir Ptuskin, Frank Jones, and Andrew Strong for discussions of various aspects of CR acceleration and propagation. An essential part of this report was prepared during a visit to the Max-Planck-Institut für extraterrestrische Physik in Garching; the warm hospitality and financial support of the Gamma Ray Group is gratefully acknowledged. This work was supported in part by a NASA Astrophysics Theory Program grant.

9. References

1. Battiston R. 2003, this conference, rapporteur talk
2. Bell A.R., Lucek, S.G. 2001, MNRAS 321, 433
3. Berezhinskii V.S., Bulanov S.V., Dogiel V.A., Ginzburg V.L., Ptuskin V.S. 1990, *Astrophysics of Cosmic Rays* (North Holland: Amsterdam)
4. Bykov A.M. 2001, *Space Science Rev.* 99, 317
5. Donato F. et al. 2001, *ApJ* 563, 172
6. Erlykin A.D., Wolfendale A.W. 1997, *Astropart. Phys.* 7, 203
7. Gleeson L.J., Axford W.I. 1968, *ApJ* 154, 1011
8. Han J.L. 2003, *Acta Astron. Sinica Suppl.* 44, 148
9. Heinbach U., Simon M. 1995, *ApJ* 441, 209
10. Hunter S.D. et al. 1997, *ApJ* 481, 205
11. Jones F.C., Ellison D.C. 1991, *Space Science Rev.* 58, 259
12. Jungman G., Kamionkowski M., Griest K. 1996, *Phys. Reports* 267, 195
13. Konstantinov A.N., Kocharov G.E., Levchenko V.A. 1990, *Sov. Astron. Lett.* 16, 343
14. Molnar A., Simon, M. 2001, in *Proc. 27th ICRC (Hamburg)*, 1877
15. Moskalenko I.V., Mashnik S.G., Strong A.W. 2001, in *Proc. 27th ICRC (Hamburg)*, 1836
16. Moskalenko I.V., Strong A.W., Ormes J.F., Potgieter M.S. 2002, *ApJ* 565, 280
17. Olinto A. 2003, this conference, rapporteur talk
18. Parker E.N. 1965, *Planet. Space Sci.* 13, 9
19. Roger R.S., Costain C.H., Landecker T.L., Swerdlyk C.M. 1999, *A&Ap Suppl.* 137, 7
20. Seo E.S., Ptuskin V.S. 1994, *ApJ* 431, 705
21. Sfeir D.M., Lallement R., Crifo F., Welsh B.Y. 1999, *A&Ap* 346, 785

- 22. Sreekumar P. et al. 1998, ApJ 494, 523
- 23. Takita M. 2003, this conference, rapporteur talk
- 24. Yanasak N.E. et al. 2001, ApJ 563, 768